Research Highlights

- Removals of superfine PAC (SPAC) and conventionally-sized PAC were examined.
- Novel image analysis method allowed visualization of particles with diameter > 0.2 μm.
- Conventional water treatment process produced a 5-log decrease in particle number.
- SPAC remained in sand filtrate at same concentration as PAC at equivalent doses.
- Smaller carbon particles were neutralized less during coagulation.

SPAC

7.5 mg/L = ~5 × 10^7 particles/mL

D_{50} = 1 µm

5.3 Log reduction

100–200 particles/mL

D_{50} = 1.5 µm

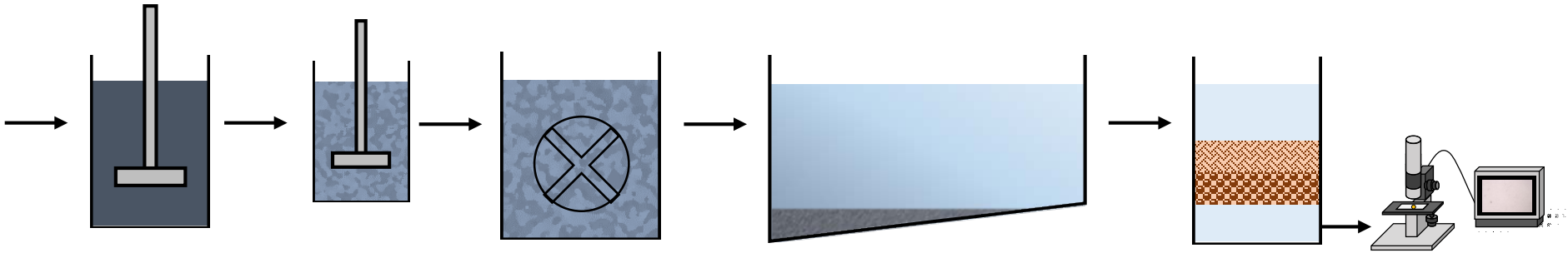

PAC

30 mg/L = ~1 × 10^7 particles /mL

D_{50} =14 µm

5.0 Log reduction

100–200 particles/mL

D_{50} = 1.5 µm

Identifying, counting, and characterizing superfine activated-carbon particles remaining after coagulation, sedimentation, and sand filtration

Yoshifumi Nakazawa [a], *Yoshihiko Matsui* [b,*], *Yusuke Hanamura* [a], *Koki Shinno* [a], *Nobutaka Shirasaki* [b], *Taku Matsushita* [b]

[a] *Graduate School of Engineering, Hokkaido University, N13W8, Sapporo 060-8628, Japan*

[b] *Faculty of Engineering, Hokkaido University, N13W8, Sapporo 060-8628, Japan*

* *Corresponding author*. Faculty of Engineering, Hokkaido University, N13W8, Sapporo 060-8628, Japan. Tel./fax: +81-11-706-7280

E-mail address: matsui@eng.hokudai.ac.jp (Y. Matsui)

ABSTRACT

Superfine powdered activated carbon (SPAC; particle diameter ~1 μm) has greater adsorptivity for organic molecules than conventionally sized powdered activated carbon (PAC). Although SPAC is currently used in the pretreatment to membrane filtration at drinking water purification plants, it is not used in conventional water treatment consisting of coagulation–flocculation, sedimentation, and rapid sand filtration (CSF), because it is unclear whether CSF can adequately remove SPAC from the water. In this study, we therefore investigated the residual SPAC particles in water after CSF treatment. First, we developed a method to detect and quantify trace concentration of carbon particles in the sand filtrate. This method consisted of 1) sampling particles with a membrane filter and then 2) using image analysis software to manipulate a photomicrograph of the filter so that black spots with a diameter > 0.2 μm (considered to be carbon particles) could be visualized. Use of this method revealed that CSF removed a very high percentage of SPAC: approximately 5-log in terms of particle number concentrations and approximately 6-log in terms of particle volume concentrations. When waters containing 7.5-mg/L SPAC and 30-mg/L PAC, concentrations that achieved the same adsorption performance, were treated, the removal rate of SPAC was somewhat superior to that of PAC, and the residual particle number concentrations for SPAC and PAC were at the same low level (100–200 particles/mL). Together, these results suggest that SPAC can be used in place of PAC in CSF treatment without compromising the quality of the filtered water in terms of particulate matter contamination. However, it should be noted that the activated carbon particles after sand filtration were smaller in terms of particle size and were charge-neutralized to a lesser extent than the activated carbon particles before sand filtration. Therefore, the tendency of small particles to escape in the filtrate would appear to be related to the fact that their small size leads to a low destabilization rate during the coagulation process and a low collision rate during the flocculation and filtration processes.

Keywords:

SPAC

PAC

image analysis

filtrate

zeta potential

1. Introduction

Recent developments in milling technology now enable the production of superfine powdered activated carbon particles (SPAC) down to micron and submicron dimensions. SPAC has an extremely fast rate of adsorption and higher capacity to adsorb dissolved organic contaminants compared with conventionally sized powdered activated carbon (PAC) (Ando et al. 2010, Bonvin et al. 2016, Dunn and Knappe 2013, Jiang et al. 2015, Matsui et al. 2015, Matsui et al. 2012, Partlan et al. 2016). To date, the majority of research dealing with SPAC has focused on its use as part of membrane filtration processes (Amaral et al. 2016, Ellerie et al. 2013, Heijman et al. 2009, Matsui et al. 2007). In membrane filtration processes, SPAC is used as an adsorbent for the removal of dissolved organic contaminants before the water is treated by membrane filtration, which removes the SPAC entirely. SPAC is already used in full-scale water treatment plants that use membrane filtration processes because dosage costs are lower for SPAC than for PAC (Kanaya et al. 2015).

SPAC may also be useful as part of conventional treatment, which consists of the following unit processes: coagulation–flocculation, sedimentation, and rapid sand filtration (CSF). However, it is possible that SPAC will be inefficiently removed in the conventional treatment compared with the treatment including membrane filtration; that is, SPAC particles might not be adequately removed during the treatment process and could then enter the distribution system.

In addition to contributing to the removal of dissolved organic contaminants, adsorbents such as PAC may affect floc formation in coagulation and flocculation processes. Younker and Walsh (2016) have reported that the addition of PAC prior to the addition of a coagulant ($FeCl_3$) reduces floc size but has little impact on the final turbidity after sedimentation. Aguilar et al. (2003) have reported that the use of PAC decreases the number of particles remaining after

coagulation-flocculation and sedimentation. In a coagulation-membrane filtration study, the addition of SPAC or PAC enhanced floc formation, and at the same dose, larger, more permeable floc particles were formed with SPAC than with PAC because of the fractal effect and the increased frequency of particle–particle collisions with SPAC (Matsui et al. 2009). These results thus suggest that the addition of SPAC may have positive effects on the coagulation–flocculation process because the carbon particles serve as nuclei for flocculation. However, if carbon particles are to serve as nuclei, their high negative charge must be neutralized; non-neutralized carbon particles do not flocculate and would pass through the sand filter into the treated water.

The effects of the addition of PAC on the turbidity of treated water after CSF were reported more than 25 years ago. Some studies reported that PAC at concentrations up to 30 mg/L did not compromise the quality of the treated water in terms of particulate matter contamination (Carns and Stinson 1978, Gifford et al. 1989). However, in those studies the quality of the filtered water was evaluated via a naked-eye visual assessment. Therefore, the number of PAC and SPAC particles remaining in treated water at concentrations below the limit of visual detection remains unknown, despite the fact that PAC in treated water at concentrations below the limit of visual detection can lead to complaints from customers such as food-processing companies and photo-finishing stores (American Society of Civil Engineers and American Water Works Association 1998, Bureau of Waterworks Tokyo Metropolitan Government 2014). Therefore, the removal of SPAC, which has a much smaller particle diameter than PAC, is a critical issue that must be addressed before SPAC is used in CSF water treatment plants.

In the present study, we developed a method for identifying and quantifying very low concentrations of SPAC (<1 μg/L, <1000 carbon particles/mL) in treated water, and we determined the concentration and characteristics of the carbon particles remaining after CSF.

2. Materials and methods

2.1. Carbon particles and coagulant

A commercially available wood-based PAC (Taiko W; Futamura Chemical Co., Ltd., Nagoya, Japan) was prepared as a slurry in pure water (Milli-Q water; Millipore, Billerica, MA, USA) and then pulverized to produce SPAC slurries of different particle sizes (Table 1). $SPAC_L$ was produced with a closed-chamber ball mill (Nikkato, Osaka, Japan) with 5- and 10-mm-diameter balls. $SPAC_{S1}$ and $SPAC_{S2}$ were produced using a bead mill with a re-circulation system (LMZ015, Ashizawa Finetech, Chiba, Japan) and 0.3-mm-diameter ZrO_2 beads (Pan et al. 2017). Standard carbon particle suspensions with predetermined mass concentrations were prepared by diluting a SPAC/PAC slurry with Sapporo City tap water filtered through a PTFE (polytetrafluoroethylene) membrane (nominal pore diameter, 0.1 μm; ϕ90 mm; Toyo Roshi Kaisha, Ltd., Tokyo, Japan). Membrane-filtered tap water without the addition of carbon particles was used as blank water. The particle size distributions of the carbons were determined by using a laser light diffraction and scattering method (Microtrac MT3300EXII, Nikkiso Co., Tokyo, Japan). To measure the true particle size distribution of the carbon particles, a sample of the slurry was pretreated by the addition of a dispersant (Triton X-100; Kanto Chemical Co., Tokyo, Japan; final concentration, 0.08% w/v) and subjected to ultrasonic dispersion before determination of the particle size distribution via the laser light diffraction and scattering method. The apparent particle size distributions of the carbon particles were measured via the same method but without dispersant addition or ultrasonic dispersion.

Poly-aluminum chloride with a basicity of 50% and sulfate content of 3% (Taki Chemical Co., Ltd, Hyogo, Japan), a coagulant widely used in water treatment plants, was used as the coagulant in this study.

123

124 *2.2. Coagulation–flocculation, sedimentation, and rapid sand filtration*

125 Tap water in Sapporo city was filtered through a membrane filter (nominal pore diameter, 0.1
126 μm; Toyo Roshi Kaisha, Ltd.) and then added with one of the carbon slurries to 30-mg/L SPAC,
127 7.5-mg/L SPAC, or 30-mg/L PAC to prepare raw waters. Most CSF experiments were
128 conducted with these waters, but two CSF experiments were conducted with water from the
129 Toyohira River (Hokkaido) after supplementing the water with SPAC at 7.5 mg/L. The river
130 water was sampled at the location where it becomes the raw water source for the Moiwa Water
131 Purification Plant (Sapporo, Japan).

132 A schematic of the experimental setup and procedure is shown in Fig. 1S (SI, Supplementary
133 Information). The coagulation–flocculation and sedimentation steps were conducted in a 4-L
134 rectangular beaker. After a predetermined volume of HCl or NaOH (0.1 N) was added to adjust
135 the coagulation pH to 7.0, the coagulant (poly-aluminum chloride) was injected into the beaker
136 to a final concentration of 4 mg-Al/L. The water was stirred rapidly for 20 s (coagulation; G =
137 600 s^{-1}, 197 rpm) and then slowly for 20 min (flocculation; 5 min at 50 s^{-1}, 38 rpm; 5 min at
138 20 s^{-1}, 20 rpm; 10 min at 10 s^{-1}, 13 rpm). The water was then left at rest for 1 h until the floc
139 particles settled. Next, the top three liters of the water (supernatant) were transferred to another
140 beaker for the determination of turbidity (2100Q portable turbidimeter; Hach Co., USA) and
141 for rapid sand filtration. The rapid sand filtration was conducted for 40 min at a rate of 90 m
142 d^{-1} in the down-flow direction using a column (ϕ4 cm) filled to a depth of 50 cm with sand
143 (effective diameter, 0.6 mm; uniformity, 1.3). The sand filtrate was collected from 13 to 40 min
144 after the start of filtration, and the turbidity and particle count of the filtrate were determined.

After each filtration run, the sand filter was backwashed with tap water for 1 h. Next, pure water (Milli-Q water) was passed through the sand filter for 1 h in the down-flow direction, followed by 3 L of membrane-filtered tap water, also in the down-flow direction. After the 3 L of membrane-filtered tap water was passed through the sand filter, the sand filtrate was collected. The particle count of the sand filtrate was always low (< 6 particles/mL), but this count was subtracted from the particle count of the filtrate collected in the filtration experiments to yield the net count of particles that had passed through the filter. The filter was then used for the next filtration experiment.

2.3. Membrane filtration and microscopic image analysis

To sample the carbon particles in the water, the water was filtered through a PTFE membrane filter (nominal pore diameter, 0.1 μm; ϕ25 mm; Millipore) supported by a glass filter holder (KG-25; Toyo Roshi Kaisha, Ltd.) (Fig. 2S, SI). After drying the filter, color digital photomicrographs were captured for nine predetermined observation zones (microscope view area, 247 × 330 μm) per filter (Fig. 3S, SI) with a digital microscope (VHX-2000; Keyence, Japan) at 1000× magnification. The photomicrographs were analyzed by using the image analysis software supplied with the microscope.

Figure 1 shows two representative image analysis series. Series A shows the image analysis of a membrane through which 100 mL of standard suspension containing 1-μg/L $SPAC_{S1}$ was filtered. Series B shows an image analysis of a membrane through which a sample of sand filtrate was filtered at a pilot-scale plant where surface water was treated by CSF after the addition of PAC (Yamaguchi et al. 2016). Panels A1 and B1 are the original photomicrographs of the surface of the membranes. In the photomicrographs, the black and dark gray spots in the background of the membrane texture are presumably carbon particles; very few of these colored spots were observed in the present study. After removal of the membrane texture, the images

were converted to grayscale (Panels A2 and B2). The black and dark gray spots in the images were identified as carbon particles based on their lightness, with the cut-off value being 195 ± 15 in the range 0–255, because the maximum lightness of carbon particles in these photographs was ~195. Touching or overlapping spots were separated from each other by using a shrink-and-blow process in the software. Spots with a diameter > 0.2 μm were individually identified. Panels A3 and B3 show detected spots, which appear black in these panels. The original photomicrograph was then checked to confirm that the spots were present in both the photomicrograph and the processed image: false spots were removed through this process. Panels A4 and B4, which show the verified spots, were then obtained. Note that if many spots with colors but not black-and-white had been observed in the photomicrographs, more advanced image processing would have been required to identify the carbon particles (see Figs. 4S and 5S, SI). However, because the raw waters used in the present study were made by adding carbon particles to membrane-filtered water or low-turbidity river water, colored spots were not observed (Fig. 1). This was true even in the photomicrographs of the samples collected at the pilot-scale water treatment plant. In principle, however, it is hard to distinguish between carbon particles and black mineral particles, but the interference due to black mineral particles would be small because of its very low concentration compared with carbon particle concentration (Figs. 6S, SI).

For each filter, the spot counts for the nine observation zones (Figs. 7S and 8S, SI) were summed to give the total spot count for the nine observation zones. The spot count for each whole filter was obtained by multiplying the total count by the ratio of the filtration area to the total area of the nine observation zones.

The filtration and counting processes were conducted three times for each water sample. The spot counts for the three filters were then averaged and corrected by subtracting the spot count

of the blank water. Dividing the average-minus-blank count by the volume of the water sample gave the carbon particle number concentration.

The volume of each particle was calculated by assuming the particle to be spherical with a diameter equal to the projected area diameter of its spot on the photomicrograph. The number concentration was converted to a volume concentration by using Eq. (1):

$$\emptyset = C_N \int_0^\infty \frac{\pi}{6} d^3 f_N(d) dd \qquad (1)$$

where $\emptyset$ is the volume concentration (dimensionless), C_N is the number concentration (cm^{-3}), d is the particle diameter (cm), and $f_N(d)$ is the particle size distribution by number (cm^{-1}).

When determining the volume concentration and the particle size distribution by volume, a blank correction was not performed. Not performing a blank correction did not substantially increase the analytical error, because the black spots observed for the blank water were very small in size and number compared to the black spots determined to be carbon particles in the water samples.

2.4. Measurement of zeta potential

The zeta potential of the carbon particles in the water samples after each stage of the water treatment process (i.e., coagulation, sedimentation, and rapid sand filtration) was determined by using a zeta electrometer (Zetasizer Nano ZS; Malvern, United Kingdom). Before the zeta potentials of the sand filtrate samples were determined, the samples were concentrated by a factor of 15.6. The zeta potentials of the other samples were measured without concentration.

To concentrate the sand filtrate samples, a tube containing 38.5 mL of sample water was centrifuged at 32,000 rpm (170,000 *g*) for 35 min at 25 °C (Ultracentrifuge L-80 XP; Beckman Coulter, USA). After centrifugation, the upper 26 mL of water in the tube was carefully removed, the tube was replenished with another 26 mL of sample water, and the tube was centrifuged again. This series of operations was repeated six times.

2.5. Fractionation of SPAC and PAC according to particle size

The SPAC in suspension (8.3 g/L) was fractionated by means of centrifugation. A tube containing 30 mL of the SPAC suspension was centrifuged for 60 min at 0, 500, 1500, or 4000 rpm (himac CT6E; Hitachi Koki Co., Ltd., Tokyo, Japan). The upper 20 mL of the sample in the tube was then withdrawn, and the particle size distribution (Microtrac MT3300EXⅡ) and zeta potential (Zetasizer Nano ZS) of the carbon particles remaining in the upper 20 mL of the sample were determined. Before measurement of the zeta potential, the turbidity of the sample was adjusted to 30 nephelometric turbidity units (NTUs) by diluting the sample with filtered tap water. Particle size distributions were determined without the addition of a dispersant or the use of ultra-sonication.

PAC in suspension (33 g/L) was fractionated by means of gravity settling. An aliquot (40 mL) of the PAC suspension was left at rest in a beaker for 0, 6, 120, or 720 min. The upper 4 mL of the sample was then withdrawn, and the zeta potential and particle size distribution were determined as described above.

3. Results and Discussion

3.1. Identification and enumeration of carbon particles on the filter

The particle concentrations in the blank water and standard suspensions (0.1, 1.0, and 10 μg/L) were determined by using the membrane-filtration and microscopic-image-analysis method (Fig. 9S, SI). The particle counts for the three blank water samples were very low, and the counts likely included false positives arising from the texture of the membrane filter and contamination. The counts in the 100-mL blank water samples were <6 particles/mL. The counts for the same standard suspensions were comparable between filters. Particle concentrations >>6 particles/mL in a 100-mL filtered water sample could therefore be easily measured.

Normalized standard deviations (coefficients of variation, C_V) of particle number concentrations were calculated for the counts of the three filters for each water sample. The C_V values for all of the measurements were collected and plotted against the mean particle number concentrations. Figure 2 shows the results for a filtration volume of 100 mL (the results for filtration volumes of 500 and 10 mL are shown in Fig. 10S, SI). The C_V decreased with increasing particle number concentration, roughly in agreement with the theoretical relationship calculated by Eq. (4), which was derived by assuming the particle count to be a Poisson-distributed random variable. The expected value and variance of a Poisson-distributed random variable are equal. Therefore, the coefficient of variation is

$$C_V = 1/\sqrt{\lambda}, \qquad (2)$$

where C_V is the coefficient of variation and λ is the mean particle count.

The particle number concentration was calculated from the mean particle count by using

$$C_N = \frac{\lambda \times a_\mathrm{f}/a_\mathrm{o}}{V}, \qquad (3)$$

where C_N is the number concentration (cm^{-3}), a_f is the filtration area (cm^2), a_o is the total area of the nine observation zones (cm^2), and V is the filtration volume (cm^3).

Substituting Eq. (3) into Eq. (2) gives

$$C_V = \sqrt{\frac{a_f/a_o}{C_N V}}. \qquad (4)$$

The observed C_V values were all less than 0.4, with the exception of one sample for which the particle number concentration was 3 particles/mL. The C_V values were <0.2 for all the samples with particle number concentrations > 200 particles/mL, which is equivalent to a SPAC concentration of > 0.07 μg/L, but the C_V values varied between samples. The C_V values of some particle number concentrations were higher than predicted by the Poisson distribution, perhaps because sintered glass filter holder (nominal pore diameter, 30–50 μm, according to the manufacturer; Fig. 11S, SI). As a result, the filtration velocity across the membrane was uneven at the microscopic level, and the volumes of water passing through the filter at the observation zones were not exactly equal. Nevertheless, the fact that the number concentrations of the standard suspensions obtained by the membrane-filtration and microscopic-image-analysis method were linearly correlated with the mass concentrations (R^2 = 1.00; Fig. 12S, SI) supports the validity of the method.

Figure 3 compares the volume-based particle size distributions of the standard carbon suspensions obtained by using our membrane-filtration and microscopic-image-analysis method with those obtained by using the laser light diffraction and scattering method. The median diameter obtained by our method was in agreement with that by the laser light

diffraction and scattering method. However, the ranges of the particle size distributions were not in good agreement. The poor agreement in particle size distribution could be due to the error generated when a number distribution of a wide distribution was converted into a volume distribution (Allen 2013). Our method measures number distribution so that it could not be accurate for large particles, which influence the volume-based size distributions to a much greater extent than small particles, because they are small in number. On the other hand, the laser light diffraction and scattering method could not be accurate in measuring small particles because smaller particles scatter light with weaker intensity.

3.2. Comparison of SPAC and PAC remaining after treatment

The turbidities, carbon particle number concentrations, and carbon particle volume concentrations for raw waters and sand filtrates are shown in Fig. 4 (the turbidities of the supernatants are shown in Fig. 13S, SI). The raw waters contained 30-mg/L PAC, 30-mg/L $SPAC_{S2}$, or 7.5-mg/L $SPAC_{S2}$. The turbidities of the sand filtrates were all very low (~0.05 NTU); the turbidities were almost the same as the turbidity observed for Milli-Q water (0.05 NTU). The false turbidity due to stray light in the turbidity measurement is < 0.02 NTU, according to the specifications of the turbidity meter. Turbidity measurements could therefore not differentiate carbon particle concentrations in the filtrates possibly containing SPAC and PAC. However, clear differences were observed in the particle number and volume concentrations determined by the membrane-filtration and microscopic-image-analysis method. A comparison of the results for raw waters containing 30 mg/L of carbon particles revealed that the SPAC number concentrations in the sand filtrate were 600–1000 particles/mL, about five times higher than the PAC number concentrations of 100–200 particles/mL. For the raw waters, the SPAC number concentrations were one order of magnitude higher than the PAC number concentrations. Therefore, the removal rates in terms of number concentration were comparable for SPAC and PAC, and that removal rates were roughly 5-log. The volume concentrations in

300 sand filtrates were higher for SPAC than for PAC. The removal rates in terms of volume
301 concentration were around 6-log for SPAC, but they were somewhat lower for PAC.

302 It has been reported that the dose of SPAC is 25% of the PAC dose needed to provide a given
303 adsorptive removal rate of a target compound, such as 2-methylisoborneol (Kanaya et al. 2015,
304 Matsui et al. 2007, Matsui et al. 2005, Matsui et al. 2013). We therefore compared the
305 experimental results obtained for raw waters containing 7.5-mg/L SPAC with those obtained
306 for raw waters containing 30-mg/L PAC. The comparison revealed that the particle number
307 concentrations in the sand filtrates were comparable (100–200 particles/mL). The particle
308 volume concentrations were also comparable (~100 μm^3/mL), although the removal rate in
309 terms of particle volume concentration was lower for SPAC than for PAC. Moreover, the
310 removal rate in terms of particle number concentration was somewhat higher for SPAC than
311 for PAC, but the difference was small (5.3-log for 7.5-mg/L SPAC and 5.0-log for 30-mg/L
312 PAC). Therefore, the concentration of carbon particles that pass through a sand filter would be
313 no higher in practice if SPAC were used instead of PAC.

314 The above-described high removals of SPAC particles were obtained in the experiments that
315 involved the use of raw waters made from filtered tap water. When the raw water of CSF
316 experiment was made from river water, the removal rate of carbon particles was similarly high,
317 5.3-log (Fig. 14S, SI). The natural suspended solids and the organic matter contained in the
318 river water before adding SPAC did not substantially affect the removal rate of SPAC particles,
319 but this result could reflect the fact that the concentrations of natural suspended solids and
320 organic matter were low (turbidity 5.7 NTU, dissolved organic carbon 0.9 mg-C/L). SPAC of
321 7.5-mg/L, by way of comparison, resulted in a turbidity of 54 NTU.

322 If the principal mechanism responsible for carbon particle removal via coagulation is charge
323 neutralization (Letterman and Yiacoumi 2011), the coagulant dosage required to remove all of

the carbon particles is determined by the total external surface area of the carbon particles (Dentel 1988, Stumm and O'Melia 1968). The total external surface area of 7.5-mg/L SPAC was similar to that of 30-mg/L PAC (Table 1S, SI). The similarity of the particle number concentrations in raw waters treated with 7.5-mg/L SPAC and 30-mg/L PAC may be due to the similarity of the total external surface areas. However, further studies are needed to better understand the effect of carbon particle size on the carbon particle concentrations in the treated water.

3.3. Characteristics of carbon particles remaining in the sand filtrate

Figure 5 shows the particle size distributions of carbon particles in raw water and sand filtrate. Compared to the raw water, the particle size distribution of SPAC in the sand filtrate was shifted toward smaller particles, an indication that smaller particles were less efficiently removed by CSF and therefore tended to pass through the filter. This tendency was more apparent for PAC. This tendency is also consistent with the observation that more SPAC than PAC remained in the sand filtrate when the raw waters with the same mass concentration of SPAC and PAC were treated, as described in section 3.2 (Fig. 4). Because particles of smaller size tended to be less efficiently removed, the particle size distributions of PAC and SPAC in the sand filtrates would eventually become similar.

Turbidity is quantified based on the amount of light scattered by particles. Specific turbidity (turbidity normalized to volume concentration) is inversely proportional to the average particle diameter calculated from the ratio of the volume to the surface area of particles with diameters larger than the wavelength of light (Kissa 1999). The implication is that turbidity is proportional to particle concentration quantified by external surface area (external surface area concentration), which is the total external surface area of the particles divided by the volume of the suspension. For standard suspensions of PAC and SPAC, turbidities were well correlated

with external surface area concentrations (Fig. 15S, SI). The external surface area concentration of the carbon particles remaining in the sand filtrate was calculated from the data obtained for the carbon particles remaining in the sand filtrate by using the membrane-filtration and microscopic-image-analysis method. When the turbidity resulting from the carbon particles remaining in the sand filtrate was estimated from the regression equation (Fig. 14S, SI) and the calculated external surface area concentration, the turbidity ranged from 2×10^{-5} to 3×10^{-4} NTU (Table 2S, SI). These values were much smaller than the turbidities actually observed for the sand filtrates (~0.05 NTU, Fig. 4). It is therefore reasonable that turbidity measurement could not differentiate carbon particle concentrations in sand filtrates, as described in section 3.2.

3.4. Mechanisms for lower removal rate of smaller carbon particles

The main mechanism underlying rapid sand filtration is interception. When particles follow streamlines which lie very close to the surface of sand grains, the particles contact the surface of the sand grains and are captured. The probability of particles coming into contact with sand grains decreases as particle size decreases (Ives 1975). According to orthokinetic aggregation theory, particle–particle collisions during flocculation occur less frequently as particles become smaller (Ives 1978). Therefore, the lower removal efficiency of small carbon particles during CSF can be explained by the interception and orthokinetic aggregation mechanisms.

To determine whether the lower removal efficiency of small carbon particles was due solely to the interception and orthokinetic aggregation or was also related to other characteristics of the carbon, a further investigation was conducted. Even if carbon particles are transported to the surface of sand grains, they are not captured if there are strong electrokinetic repulsive forces between the sand grains and the carbon particles. Particle–particle collisions do not result in aggregation if significant repulsion exists. We therefore examined the zeta potential of the

carbon particles, a commonly used index of the electrokinetic potential in colloidal dispersions or aggregations that is correlated with coagulation and filtration performance. Figure 6 shows the zeta potential of carbon particles in raw water, water sampled after coagulation, supernatant after sedimentation, and sand filtrate. The zeta potential of the carbon particles in the raw water was approximately −23 mV, but it increased to −4 ± 8 mV after coagulation, an indication that the charge on the carbon particles had been almost fully neutralized during the coagulation process. However, the particles remaining in the supernatant had a higher negative charge (−9 ± 5mV) than the particles after coagulation. The particles in the sand filtrate, which were smaller in size than the particles before CSF, had a higher negative charge (−15 ± 5mV) than those in the supernatant.

The zeta potentials of the untreated SPAC and PAC particles did not vary as a function of particle size. Figure 7 shows the zeta potentials of the carbon particles as a function of carbon particle size. SPAC and PAC were separated by particle size based on the differences in the settling velocities of the particles. The original SPAC and PAC particles had a similar zeta potential of −20 to −25 mV. The negative charge was slightly higher for particles with a diameter of 3 μm, and it then decreased with decreasing particle size, although the decrease was small. The reason for this small change in charge is unclear; however, the data indicate that the smaller carbon particles were not intrinsically higher negatively charged than the larger carbon particles, and the surface charges were not very different between the large and small carbon particles. However, the small carbon particles that remained in the sand filtrate had a higher negative charge than the carbon particles after coagulation. Therefore, the small carbon particles were charge-neutralized and destabilized at a lower rate than large carbon particles during the coagulation process. A possible explanation for the weak neutralization of the small particles during the coagulation process is that the adsorption of aluminum hydroxide species onto particles is a transport-limited process that depends on the particle size, and the rate of

adsorption onto small particles is low (Elimelech et al. 1995, Gregory 1988). Finally, we conclude that the low destabilization rate during the coagulation process, the low frequency of particle–particle collisions during flocculation, and the low probability of the particles coming into contact with sand grains during the sand filtration process could collectively make it difficult for small carbon particles to be removed by CSF, the result being that small carbon particles tended to remain in the sand filtrate.

4. Conclusions

We developed a method to detect and measure the number of carbon particles remaining in sand filtrate. The method used membrane filtration, digital microscopy, and image analysis. We used this method to identify carbon particles with diameters > 0.2 μm at a concentration as low as 0.1 μg/L. By using this method, we were able to determine the trace concentration of residual carbon particles in sand filtrates, concentrations far below the limit of detection by turbidity measurements.

The residual concentration of SPAC was similar to that of PAC when the SPAC was used at 25% of the PAC mass concentration, a percentage that resulted in comparable adsorption of dissolved organic contaminants by SPAC and PAC (SPAC mass dose is 25% of the PAC mass dose, but the SPAC enables comparable adsorptive removal to PAC). This result suggests that when SPAC is used instead of PAC, the risk that some activated carbon particles may pass through the CSF processes and remain in the treated water would not substantially increase. The number concentrations in the sand filtrate were 100–200 particles/mL when 7.5 mg/L SPAC and 30 mg/L PAC were treated. Reductions of approximately 5-log in terms of particle number concentrations and 6-log in terms of particle volume concentrations were attained via CSF.

Carbon particles remaining after CSF treatment were smaller in size than were the carbon particles before treatment. The small carbon particles remaining after CSF treatment had a higher negative charge than the carbon particles after coagulation treatment. The tendency of smaller particles to appear in the sand filtrate was therefore related to their lower destabilization rate during the coagulation process as well as their lower collision rates in the flocculation and filtration processes.

Acknowledgments

Funding: This work was supported by the Japan Society for the Promotion of Science [grant number 16H06362].

References

Aguilar, M.I., Sáez, J., Lloréns, M., Soler, A. and Ortuño, J.F. (2003) Microscopic observation of particle reduction in slaughterhouse wastewater by coagulation–flocculation using ferric sulphate as coagulant and different coagulant aids. Water Research 37(9), 2233-2241.

Allen, T. (2013) Particle size measurement, Springer US.

Amaral, P., Partlan, E., Li, M., Lapolli, F., Mefford, O.T., Karanfil, T. and Ladner, D.A. (2016) Superfine powdered activated carbon (S-PAC) coatings on microfiltration membranes: Effects of milling time on contaminant removal and flux. Water Research 100, 429-438.

American Society of Civil Engineers and American Water Works Association (1998) Water Treatment Plant Design, McGraw-Hill.

Ando, N., Matsui, Y., Kurotobi, R., Nakano, Y., Matsushita, T. and Ohno, K. (2010) Comparison of natural organic matter adsorption capacities of super-powdered activated carbon and powdered activated Carbon. Water Research 44(14), 4127-4136.

Bonvin, F., Jost, L., Randin, L., Bonvin, E. and Kohn, T. (2016) Super-fine powdered activated carbon (SPAC) for efficient removal of micropollutants from wastewater treatment plant effluent. Water Research 90, 90-99.

Bureau of Waterworks Tokyo Metropolitan Government (2014) Personal communication.

Carns, K.E. and Stinson, K.B. (1978) Controlling organics: The East Bay Municipal Utility District experience. Journal of American Water Works Association 70(11), 637-644.
Dentel, S.K. (1988) Application of the precipitation-charge neutralization model of coagulation. Environmental Science & Technology 22(7), 825-832.
Dunn, S.E. and Knappe, D.R.U. (2013) DBP precursor and micropollutant removal by powdered activated carbon, Water Research Foundation, Denver, CO, USA.
Elimelech, M., Gregory, J., Jia, X. and Williams, R.A. (1995) Particle Deposition & Aggregation, pp. xiii-xv, Butterworth-Heinemann, Woburn.
Ellerie, J.R., Apul, O.G., Karanfil, T. and Ladner, D.A. (2013) Comparing graphene, carbon nanotubes, and superfine powdered activated carbon as adsorptive coating materials for microfiltration membranes. Journal of Hazardous Materials 261(0), 91-98.
Gifford, J.S., George, D.B. and Adams, V.D. (1989) Synergistic effects of potassium permanganate and PAC in direct filtration systems for THM precursor removal. Water Research 23(10), 1305-1312.
Gregory, J. (1988) Polymer adsorption and flocculation in sheared suspensions. Colloids and Surfaces 31, 231-253.
Heijman, S.G.J., Hamad, J.Z., Kennedy, M.D., Schippers, J. and Amy, G. (2009) Submicron powdered activated carbon used as a pre-coat in ceramic micro-filtration. Desalination and Water Treatment 9(1-3), 86-91.
Ives, K.J. (1975) The scientific basis of filtration: proceedings of the NATO Advanced Study Institute held at Cambridge, U.K., July 2-20, 1973, Noordhoff.
Ives, K.J. (1978) The Scientific Basis of Flocculation, Springer.
Jiang, W., Xiao, F., Wang, D.S., Wang, Z.C. and Cai, Y.H. (2015) Removal of emerging contaminants by pre-mixed PACl and carbonaceous materials. RSC Advances 5(45), 35461-35468.
Kanaya, S., Kawase, Y. and Mima, S. (2015) Drinking water treatment using superfine PAC (SPAC): design and successful operation history in full-scale plant, pp. 624-631, American Water Works Association, Salt Lake City, Utah, USA
Kissa, E. (1999) Dispersions: Characterization, Testing, and Measurement, Taylor & Francis.
Letterman, R.D. and Yiacoumi, S. (2011) Water Quality & Treatment: A Handbook on Drinking Water, Sixth Edition. American Water Works, A. and James, E. (eds), McGraw Hill Professional, Access Engineering.
Matsui, Y., Aizawa, T., Kanda, F., Nigorikawa, N., Mima, S. and Kawase, Y. (2007) Adsorptive removal of geosmin by ceramic membrane filtration with super-powdered activated carbon. Journal of Water Supply: Research and Technology—AQUA 56(6-7), 411-418.
Matsui, Y., Hasegawa, H., Ohno, K., Matsushita, T., Mima, S., Kawase, Y. and Aizawa, T. (2009) Effects of super-powdered activated carbon pretreatment on coagulation and trans-membrane pressure buildup during microfiltration. Water Research 43(20), 5160-5170.
Matsui, Y., Murase, R., Sanogawa, T., Aoki, H., Mima, S., Inoue, T. and Matsushita, T. (2005) Rapid adsorption pretreatment with submicrometre powdered activated carbon particles before microfiltration. Water Science and Technology 51(6-7), 249-256.
Matsui, Y., Nakao, S., Sakamoto, A., Taniguchi, T., Pan, L., Matsushita, T. and Shirasaki, N. (2015) Adsorption capacities of activated carbons for geosmin and 2-methylisoborneol vary with activated carbon particle size: Effects of adsorbent and adsorbate characteristics. Water Research 85, 95-102.
Matsui, Y., Nakao, S., Taniguchi, T. and Matsushita, T. (2013) Geosmin and 2-methylisoborneol removal using superfine powdered activated carbon: Shell adsorption and branched-pore kinetic model analysis and optimal particle size. Water Research 47(8), 2873-2880.

Matsui, Y., Yoshida, T., Nakao, S., Knappe, D.R.U. and Matsushita, T. (2012) Characteristics of competitive adsorption between 2-methylisoborneol and natural organic matter on superfine and conventionally sized powdered activated carbons. Water Research 46(15), 4741-4749.
Pan, L., Nishimura, Y., Takaesu, H., Matsui, Y., Matsushita, T. and Shirasaki, N. (2017) Effects of decreasing activated carbon particle diameter from 30 μm to 140 nm on equilibrium adsorption capacity. Water Research 124, 425-434.
Partlan, E., Davis, K., Ren, Y., Apul, O.G., Mefford, O.T., Karanfil, T. and Ladner, D.A. (2016) Effect of bead milling on chemical and physical characteristics of activated carbons pulverized to superfine sizes. Water Research 89, 161-170.
Stumm, W. and O'Melia, C.R. (1968) Stoichiometry of coagulation. Journal of American Water Works Association 60(5), 514-539.
Yamaguchi, J., Yamaguchi, D. and Kawase, Y. (2016) Application study of superfine powdered activated carbon in coagulation, sedimentation and filtration (II), pp. 284-285, Japan Water Works Association, Kyoto, Japan.
Younker, J.M. and Walsh, M.E. (2016) Effect of adsorbent addition on floc formation and clarification. Water Research 98, 1-8.

List of Table and Figure

Table 1. Carbon particle size. The median diameters are based on the particle size distribution as determined by the laser light diffraction and scattering method.

Figure 1. Representative image analysis series. Series A begins with a photomicrograph captured of a filter through which 100 mL of standard suspension containing 1-μg/L $SPAC_{S1}$ was passed. Series B begins with a photomicrograph of a filter through which a sand filtrate of unknown carbon particle concentration was passed (the water was treated by a CFS after the addition of 20-mg/L PAC). Panels A2 and B2 are grayscale conversions of the original photomicrographs. The grayscale images were converted to a binary image (Panels A3 and B3) in which the spots were detected according to lightness. Panels A4 and B4 are images after visual verification that all of the black sports in Panels A3 and B3 were included in the original photomicrograph (panels A1 and B1); spots not found in the original photomicrograph were eliminated. The yellow circles indicate dots that were verified as not being carbon particles, which were removed during image processing. The brown circles indicate dots eliminated by checking the original photograph (Panels A1 and B1).

Figure 2. Mean particle number concentration versus cofficient of variation for a filtration volume of 100 mL/filter. The line was calculated by using equation (4), which was derived from the Poisson distribution.

Figure 3. Comparison of volume-based particle size distributions determined by means of our membrane-filtration and microscopic image analysis process and by using a Microtrac MT3300EXII instrument (laser light diffraction and scattering method; Nikkiso Co., Tokyo, Japan) without the addition of a dispersant or the use of ultrasonication. Panel A, PAC; panel B, $SPAC_L$; panel C, $SPAC_{S1}$; panel D, $SPAC_{S2}$.

Figure 4. Reduction of carbon particles by the CSF treatment. Panels A1–C1, 30-mg/L PAC; panels A2–C2, 30-mg/L $SPAC_{S2}$; panels A3–C3, 7.5-mg/L $SPAC_{S2}$. Experiments were conducted twice for each experimental condition (Run 1 and Run 2). Error bars indicate standard deviations of measurement for each experiment.

Figure 5. Particle size distributions before and after treatment. Panels A1 and B1, 30-mg/L PAC (Run 1); panels A2 and B2, 30-mg/L $SPAC_{S2}$ (Run 1). Particle size distributions were obtained by means of membrane-filtration and microscopic image analysis.

Figure 6. Changes in the zeta potential of PAC and $SPAC_{S2}$ during coagulation-flocculation, sedimentation, and rapid sand filtration. The carbon particle concentration of the initial suspension was 30 mg/L. Error bars indicate standard deviations.

Figure 7. Zeta potential and median diameter of carbon particles remaining after sedimentation (PAC) or centrifugation ($SPAC_{S2}$). Error bars indicate standard deviations.

Table 1. Carbon particle size. The median diameters are based on the particle size distribution as determined by the laser light diffraction and scattering method.

Activated carbon		Median diameter (μm)
PAC		13.7
SPAC	$SPAC_L$	2.54
	$SPAC_{S1}$	0.91
	$SPAC_{S2}$	0.96

Note: $SPAC_L$, SPAC with a large particle size; $SPAC_{S1}$ and $SPAC_{S2}$, the first and the second, respectively, batch of SPAC with a small particle size.

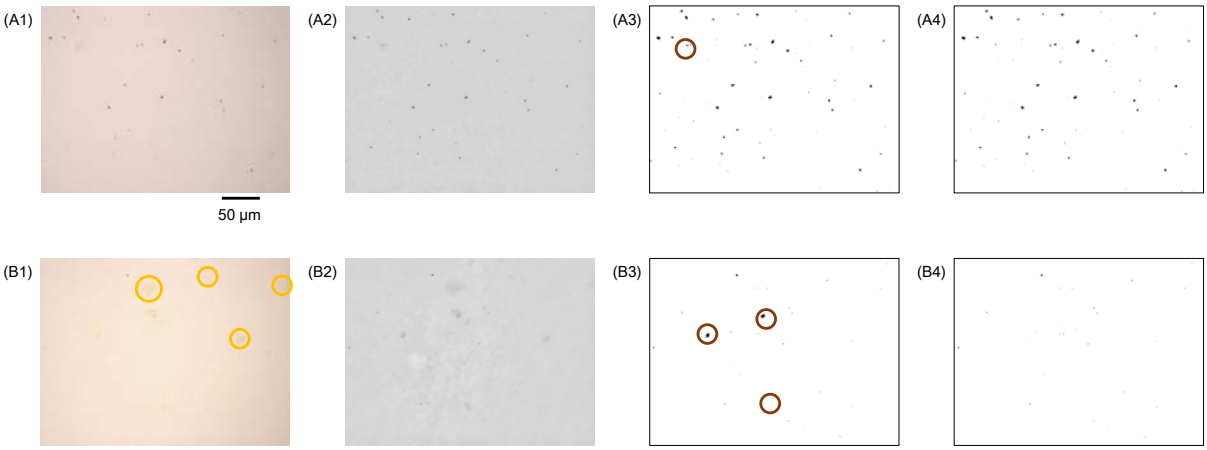

Figure 1. Representative image analysis series. Series A begins with a photomicrograph captured of a filter through which 100 mL of standard suspension containing 1-µg/L $SPAC_{S1}$ was passed. Series B begins with a photomicrograph of a filter through which a sand filtrate of unknown carbon particle concentration was passed (the water was treated by a CFS after the addition of 20-mg/L PAC). Panels A2 and B2 are grayscale conversions of the original photomicrographs. The grayscale images were converted to a binary image (Panels A3 and B3) in which the spots were detected according to lightness. Panels A4 and B4 are images after visual verification that all of the black sports in Panels A3 and B3 were included in the original photomicrograph (panels A1 and B1); spots not found in the original photomicrograph were eliminated. The yellow circles indicate dots that were verified as not being carbon particles, which were removed during image processing. The brown circles indicate dots eliminated by checking the original photograph (Panels A1 and B1).

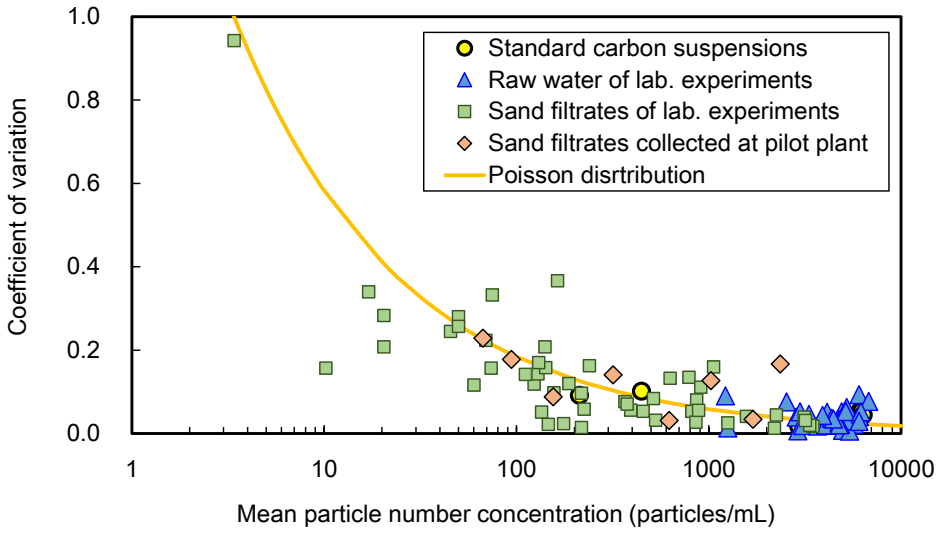

Figure 2. Mean particle number concentration versus cofficient of variation for a filtration volume of 100 mL/filter. The line was calculated by using equation (4), which was derived from the Poisson distribution.

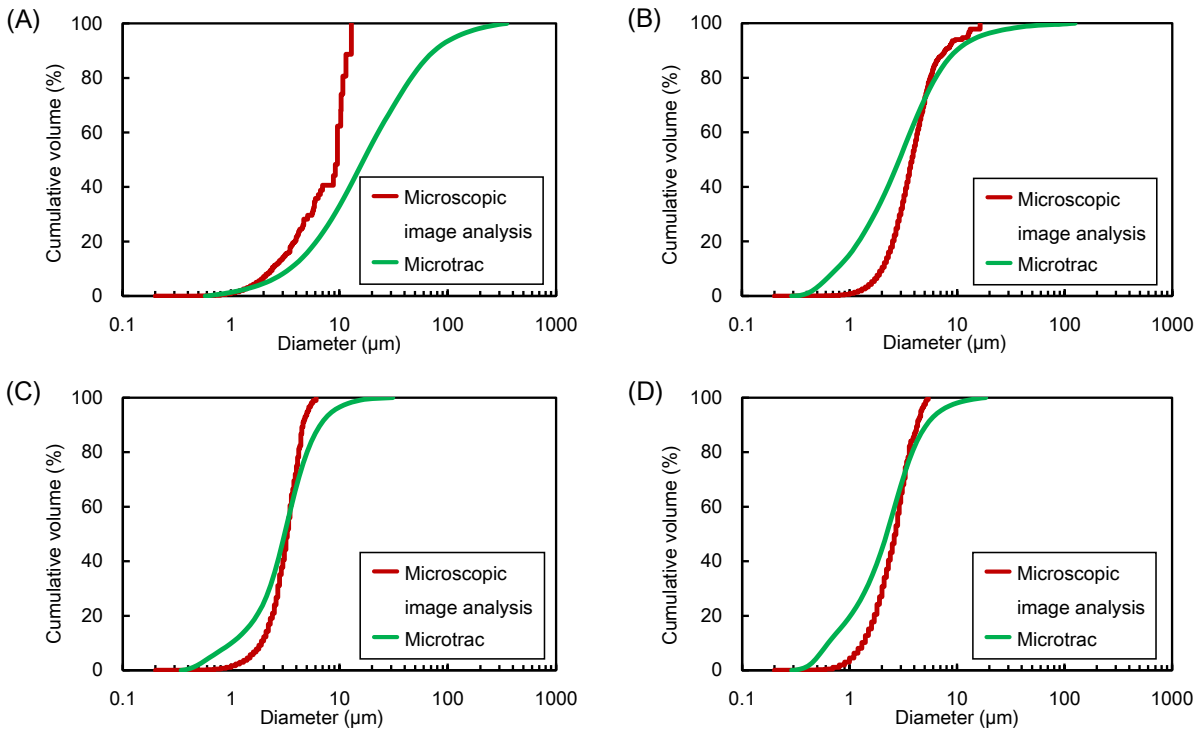

Figure 3. Comparison of volume-based particle size distributions determined by means of our membrane-filtration and microscopic image analysis process and by using a Microtrac MT3300EXII instrument (laser light diffraction and scattering method; Nikkiso Co., Tokyo, Japan) without the addition of a dispersant or the use of ultrasonication. Panel A, PAC; panel B, $SPAC_L$; panel C, $SPAC_{S1}$; panel D, $SPAC_{S2}$.

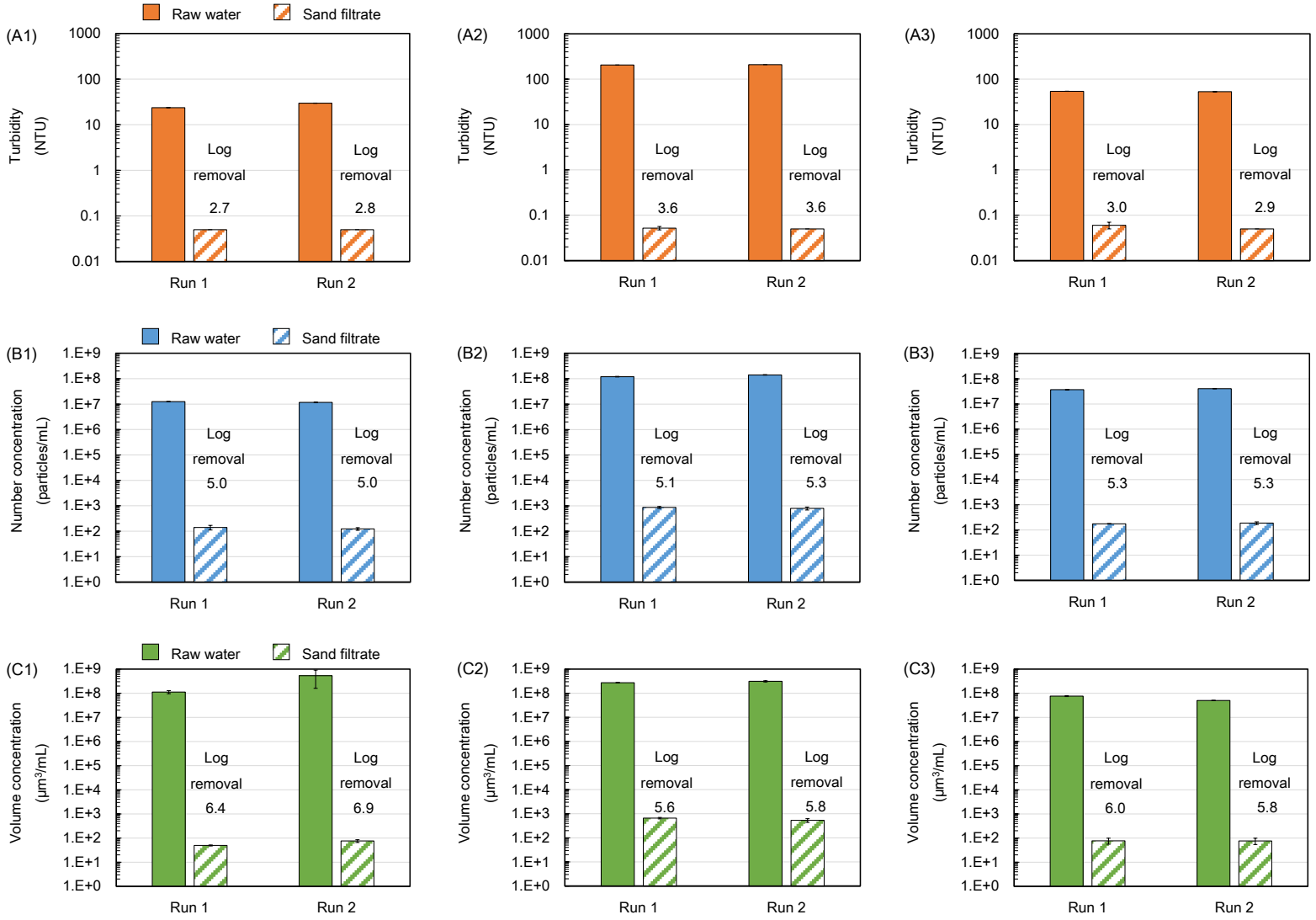

Figure 4. Reduction of carbon particles by the CSF treatment. Panels A1–C1, 30-mg/L PAC; panels A2–C2, 30-mg/L $SPAC_{S2}$; panels A3–C3, 7.5-mg/L $SPAC_{S2}$. Experiments were conducted twice for each experimental condition (Run 1 and Run 2). Error bars indicate standard deviations of measurement for each experiment.

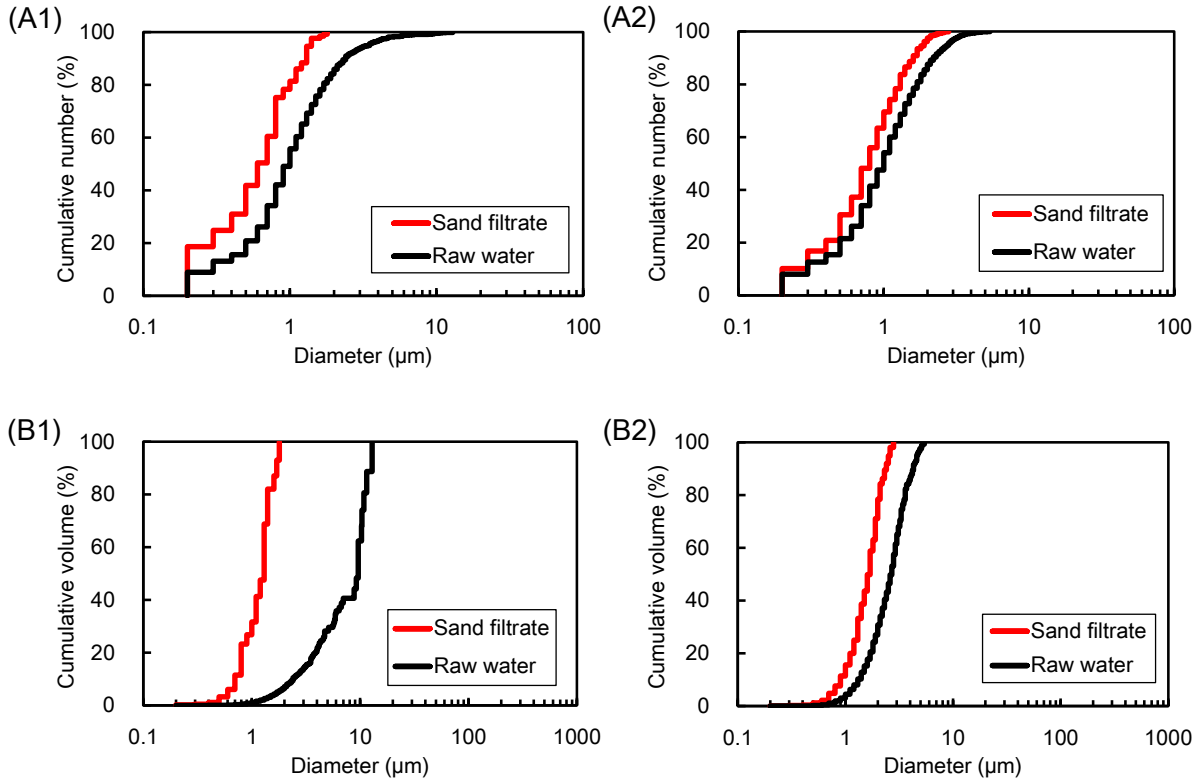

Figure 5. Particle size distributions before and after treatment. Panels A1 and B1, 30-mg/L PAC (Run 1); panels A2 and B2, 30-mg/L $SPAC_{S2}$ (Run 1). Particle size distributions were obtained by means of membrane-filtration and microscopic image analysis.

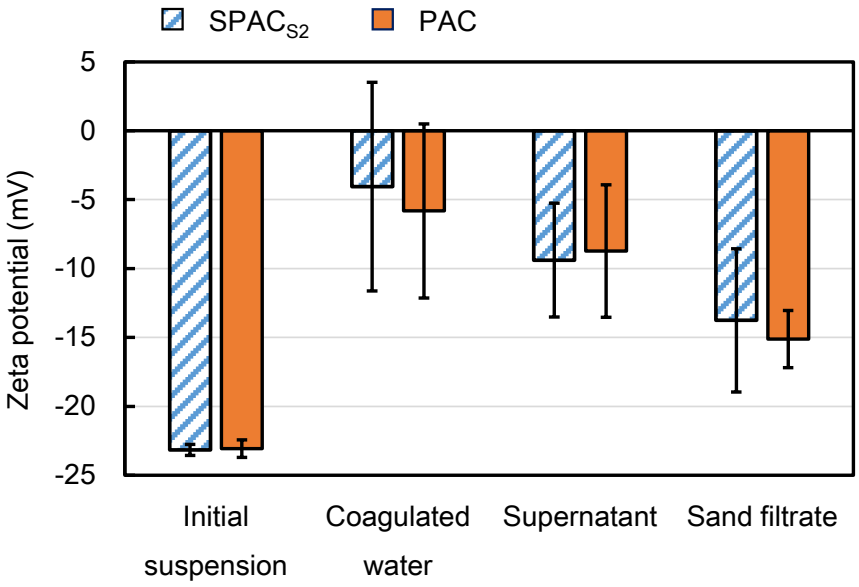

Figure 6. Changes in the zeta potential of PAC and SPAC$_{S2}$ during coagulation-flocculation, sedimentation, and rapid sand filtration. The carbon particle concentration of the initial suspension was 30 mg/L. Error bars indicate standard deviations.

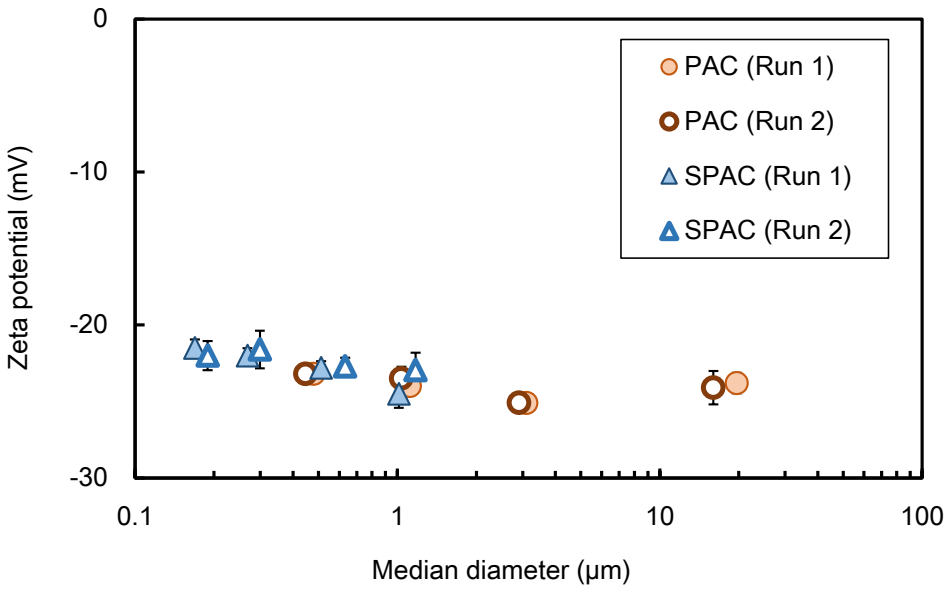

Figure 7. Zeta potential and median diameter of carbon particles remaining after sedimentation (PAC) or centrifugation ($SPAC_{S2}$). Error bars indicate standard deviations.

Supplementary Information

Identifying, counting, and characterizing superfine activated-carbon particles remaining after coagulation sedimentation and sand filtration treatment

Yoshifumi Nakazawa [a], Yoshihiko Matsui [b*], Yusuke Hanamura [a], Koki Shinno [a], Nobutaka Shirasaki [b], and Taku Matsushita [b]

a Graduate School of Engineering, Hokkaido University, N13W8, Sapporo 060-8628, Japan
b Faculty of Engineering, Hokkaido University, N13W8, Sapporo 060-8628, Japan

* Corresponding author. Tel./fax: +81-11-706-7280
E-mail address: matsui@eng.hokudai.ac.jp

Table 1S. External surface area concentration.

Activated carbon	Mass concentration (mg/L)	External surface area concentration (cm^2/L)	
		Microscopic image analysis	Microtrac
PAC	30	1.4×10^3	2.5×10^2
$SPAC_{S2}$	7.5	2.0×10^3	3.3×10^2
$SPAC_{S2}$	30	7.9×10^3	1.3×10^3

Table 2S. Estimation of turbidity arising from carbon particles remaining in the sand filtrate.

Raw water			Sand filtrate			
Activated carbon	Mass concentration	Turbidity	Turbidity	Number concentration of carbon particles	External surface area concentration of carbon particles	Turbidity attributable to carbon particles
		Turbidity meter	Turbidity meter	Microscopic image analysis	Microscopic image analysis	Estimation from external surface area concentration
	mg/L	NTU	NTU	mL^{-1}	cm^2/L	NTU
PAC	30	27	0.05	1.3×10^{2}	3.1×10^{-3}	1.9×10^{-5}
$SPAC_{S2}$	7.5	54	0.06	1.8×10^{2}	3.9×10^{-3}	2.4×10^{-5}
$SPAC_{S2}$	30	207	0.05	8.3×10^{2}	2.5×10^{-2}	1.9×10^{-4}

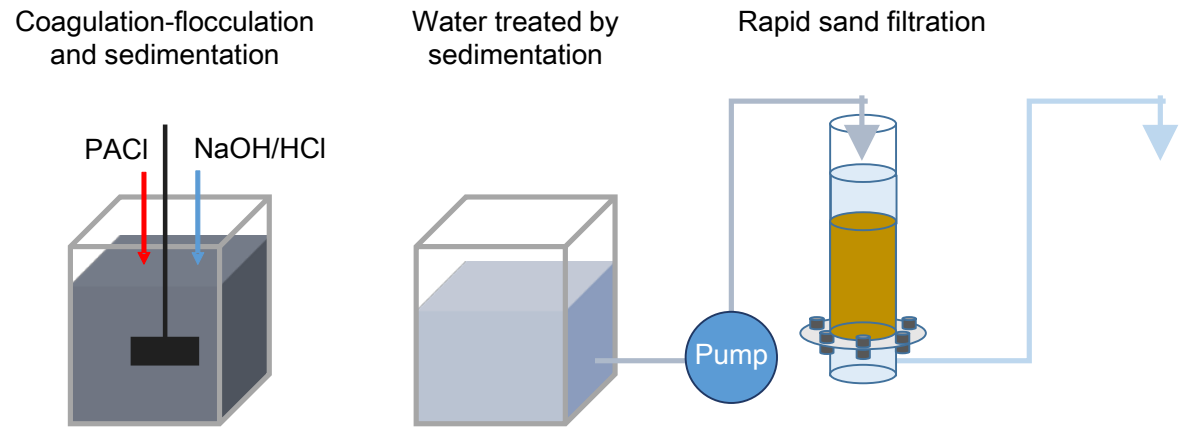

Figure 1S. Schematic diagram of the experimental setup for the coagulation-flocculation, sedimentation, and sand filtration experiment.

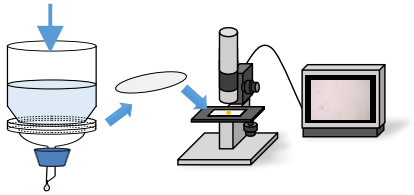

Figure 2S. Schematic diagram of the experimental setup for membrane filtration and microscopic image analysis.

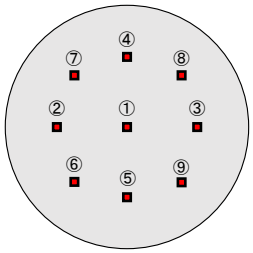

Figure 3S. Observation zones on a single membrane filter (ϕ25 mm).

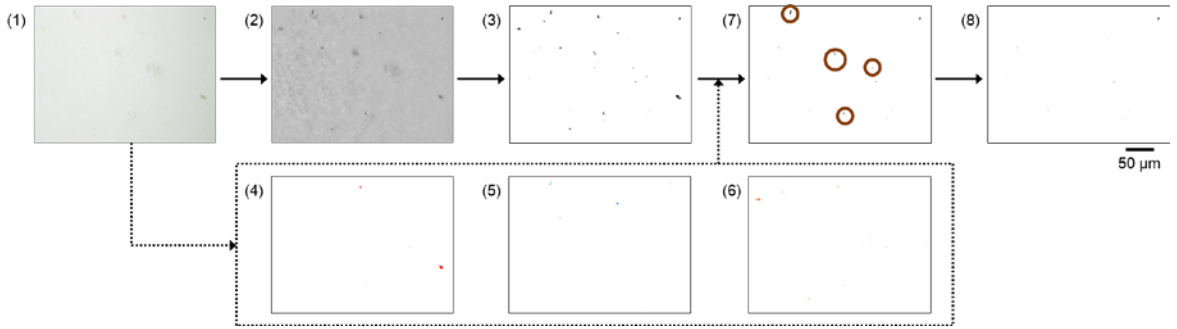

Figure 4S. Representative image analysis series showing the process when many colored spots were observed in the photomicrograph. Panel 1 is a photomicrograph of a filter through which 100 mL of water containing 0.1-µg/L $SPAC_{S2}$ and 30 µg/L of powdered mineral pigments (10 µg/L each of Iwaaka241 [red], Gunjo342 [blue], Yamabuki121 [yellow]; Nakagawa Gofun Enogu Co., Ltd., Kyoto, Japan) was passed. Panel 2 is a grayscale conversion of the original photomicrograph. The grayscale image was converted to a binary image (Panel 3) in which the spots were detected according to lightness. Panels 4, 5, and 6 are binary images in which red, blue, and yellow spots, respectively, were extracted according to their HSL (hue, saturation, and lightness). Panel 7 is the image after comparison with Panels 3 to 6 during which spots that were verified as not being black particles were eliminated. Panel 8 is the image after visual verification that all of the black spots in Panel 7 were included in the original photomicrograph (Panel 1); spots not found in the original photomicrograph were eliminated. The brown circles indicate spots that were eliminated by the visual examination.

When black and colored spots were both observed on the membrane, it was difficult to distinguish the black particles from the color particles using only lightness, particularly to distinguish black particles from blue particles, which resulted in an increase in the number of false positives. Therefore, black and colored particles were identified with the image in the HSL color model (Panels 3–7), and black particles could be distinguished from colored particles (Panel 4–7) by comparing the images (Figure 5S).

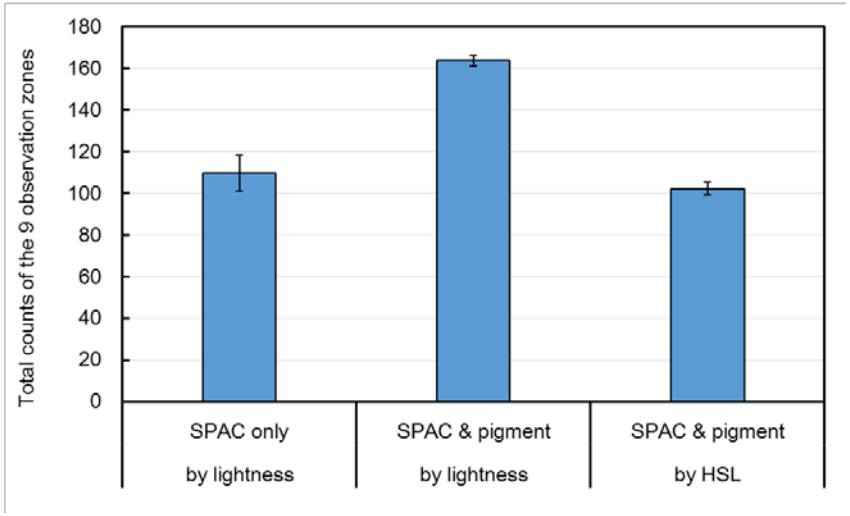

Figure 5S. Comparison of particle counts obtained for treated water originally containing 0.1-μg/L $SPAC_{S2}$ and 30-μg/L powdered mineral pigment particles (10 μg/L each of Iwaaka241 [red], Gunjo342 [blue], Yamabuki121 [yellow]; Nakagawa Gofun Enogu Co., Ltd., Kyoto, Japan).

When lightness only was used to identify carbon particles, the particle count for the suspension containing SPAC and pigments was larger than that for the suspension containing SPAC only because some of the pigment particles were erroneously counted as carbon particles. When the HSL (hue, saturation, lightness) color model was used (see Figure 4S), the counts of the suspension containing SPAC and pigment were similar to those containing SPAC, indicating that the majority of false positives were eliminated. Note that this analysis using the HSL color model still required visual examination. In the present study, however, this more advanced analysis using the HSL color model was not required because the particles in the photomicrographs were mostly black particles interspersed with a few gray particles so colored particles were hardly observed. Therefore, the detection of carbon particles according to lightness alone could be enough for analysis.

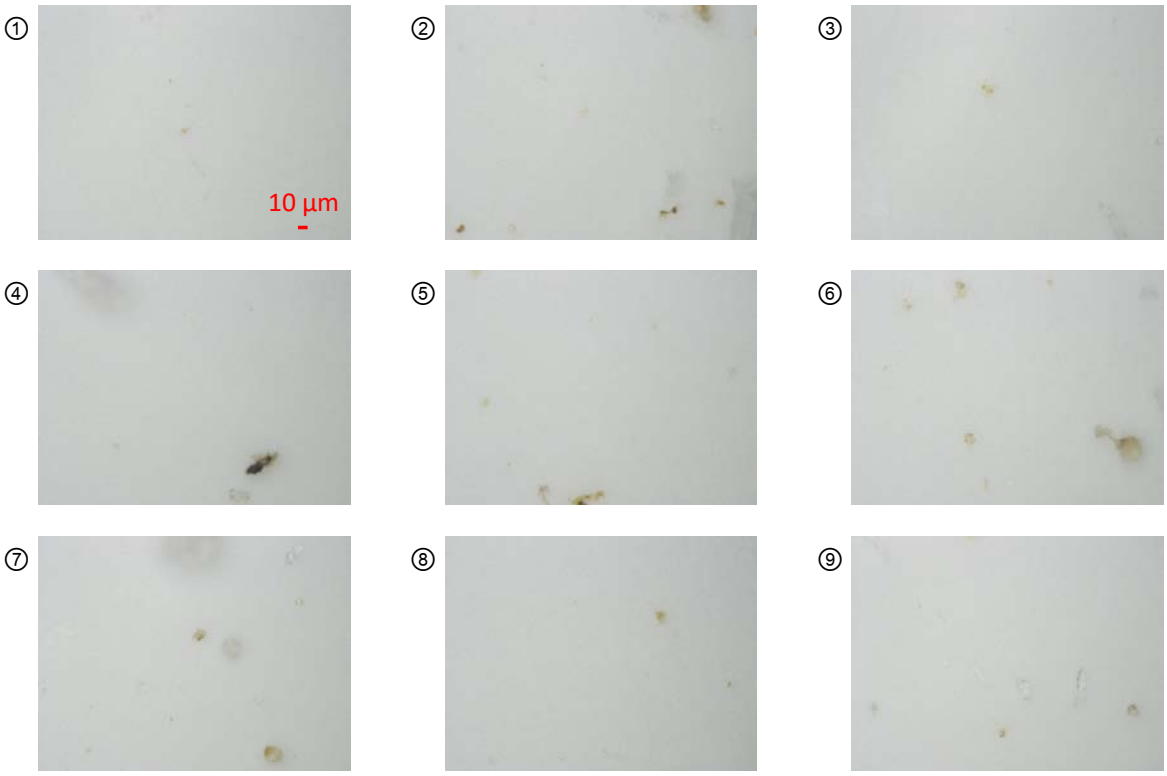

Figure 6S. Photomicrographs of nine observation zones on a filter that was passed a diluted river water (Turbidity and DOC of the river water were 5.7 NTU and 0.9 mg/L, respectively. The river water was diluted 100 times with by Milli-Q water). The concentration of black particles in the river water was 5.1×10^3 particles/mL, that was far small compared to the concentration of carbon particles. For example, 3.9×10^7 carbon particles/mL exist in $SPAC_{S2}$ suspension of 7.5-mg/L.

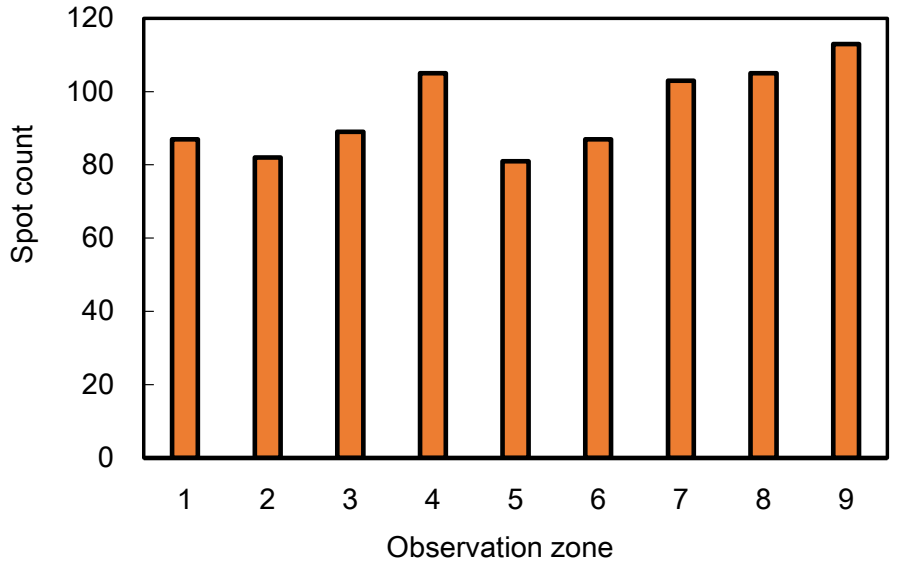

Figure 7S. Particle counts for the nine observation zones in a filter. An aliquot (100 mL) of standard suspension containing 1-μg/L $SPAC_{S1}$ was filtered through a membrane filter. The observation zone numbers correspond with those presented in Figure 3S.

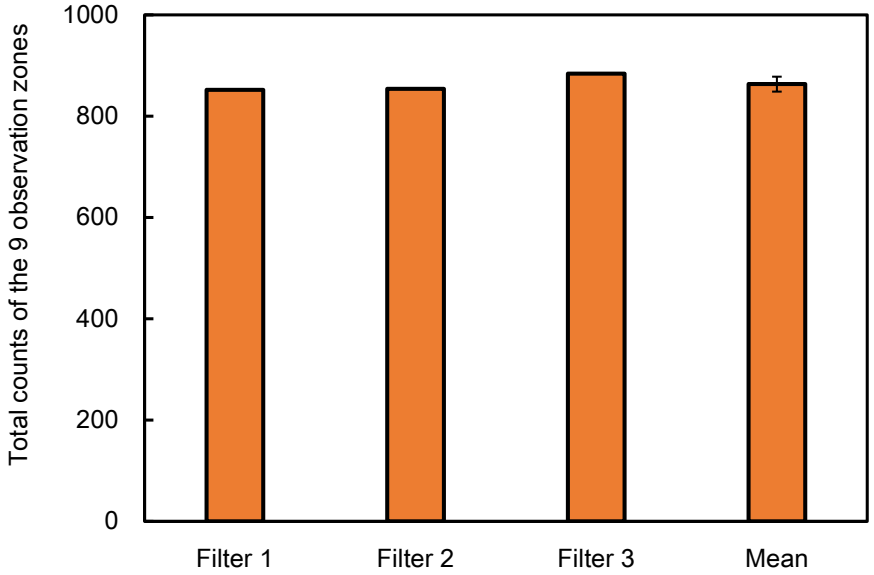

Figure 8S. Total particle counts for the nine observation zones in three filters and their mean value. An aliquot (100 mL) of standard suspension containing 1-μg/L $SPAC_{S1}$ was filtered through each filter. The error bar represents the standard deviation.

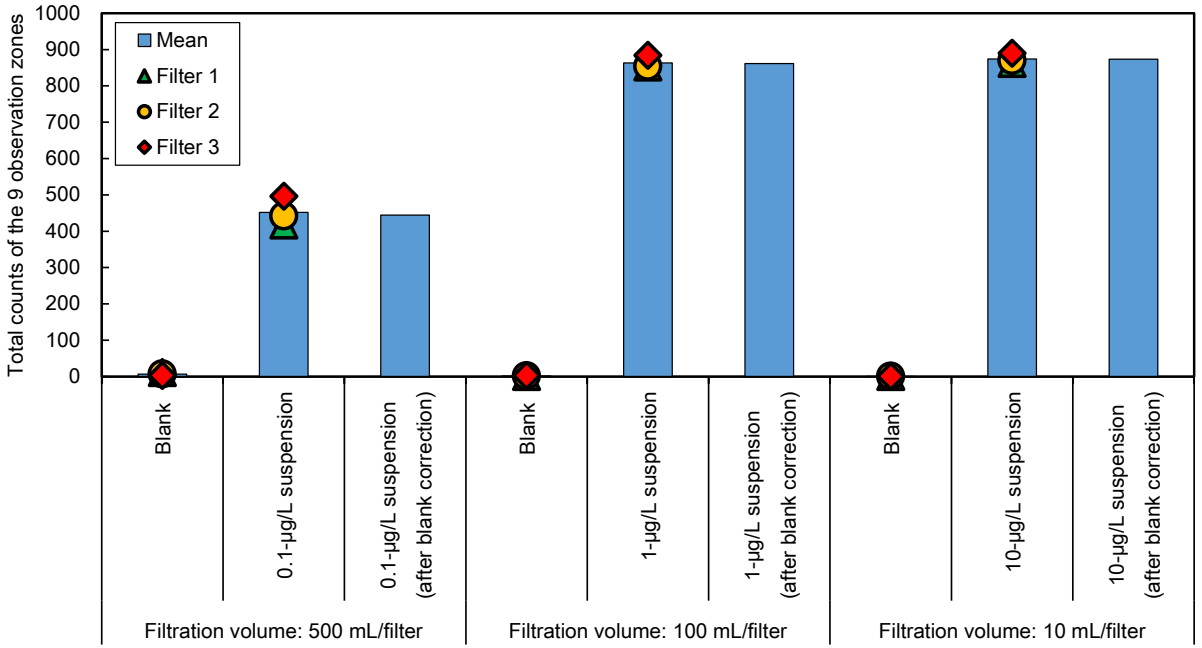

Figure 9S. Total particle counts for filters through which $SPAC_{S1}$ standard suspensions and blank water were passed.

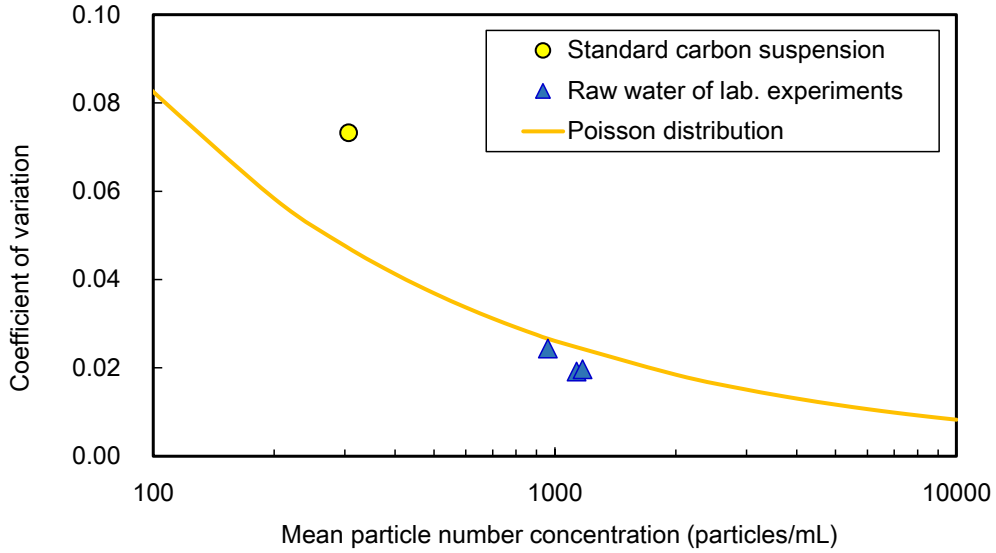
0.10
0.08
0.06
0.04
0.02
0.00
Coefficient of variation
Standard carbon suspension
Raw water of lab. experiments
Poisson distribution
100
1000
10000
Mean particle number concentration (particles/mL)

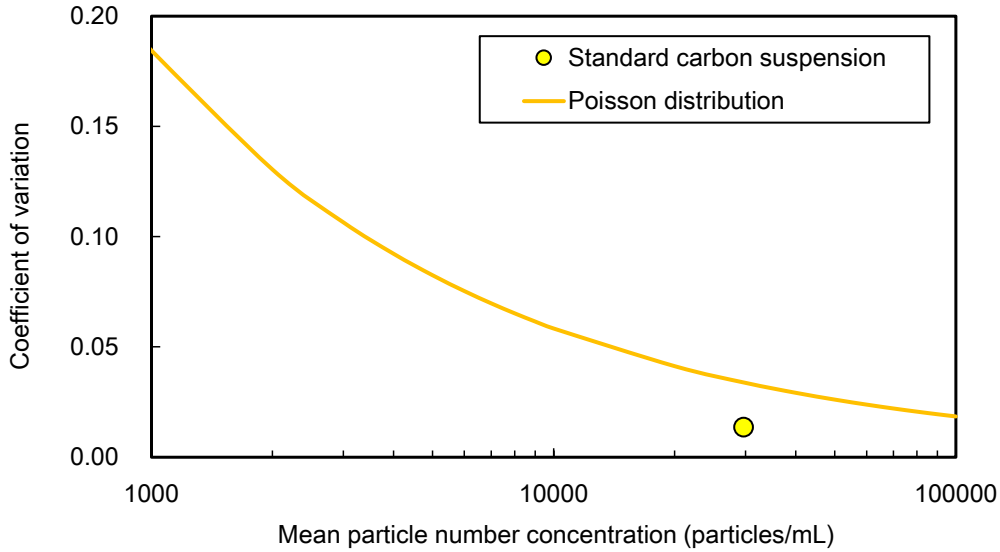
0.20
0.15
0.10
0.05
0.00
Coefficient of variation
Standard carbon suspension
Poisson distribution
1000
10000
100000
Mean particle number concentration (particles/mL)

Figure 10S. Particle number concentration mean versus coefficient of variation. Filtration volume, 500 mL and 10 mL/filter for the upper and lower panel, respectively. The lines were calculated by using equation (4), which was derived from the Poisson distribution.

Figure 11S. Photograph of the sintered glass in the filter holder.

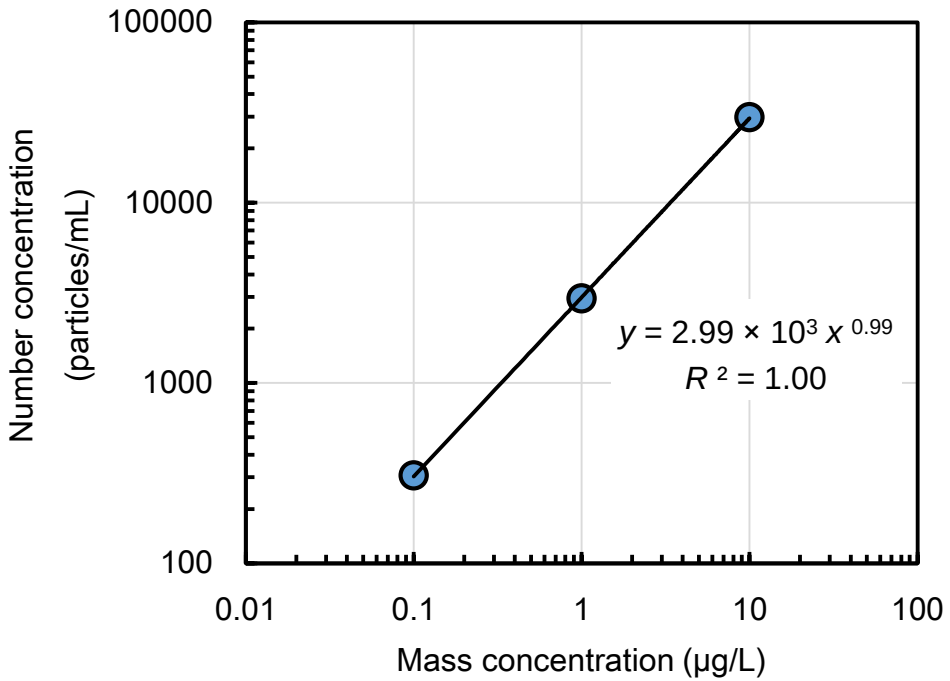

Figure 12S. Number concentration, as obtained by membrane-filtration and microscopic image analysis, versus mass concentration for the three $SPAC_{S1}$ standard suspensions. Error bars are hidden in the plot.

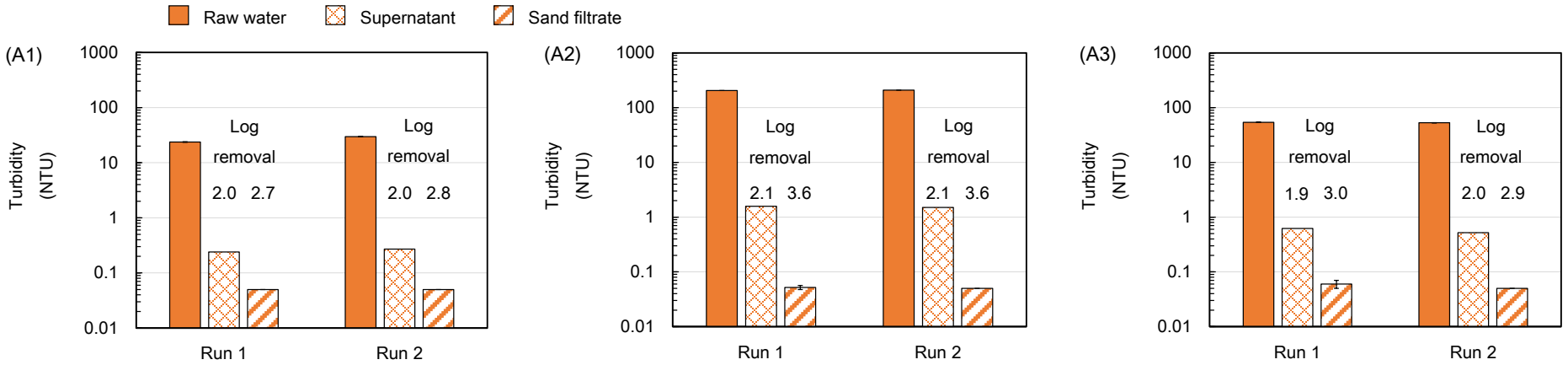

Figure 13S. Change of turbidity by coagulation-flocculation, sedimentation, and rapid sand filtration. Panels A1, 30-mg/L PAC; panels A2, 30-mg/L $SPAC_{S2}$; panels A3, 7.5-mg/L $SPAC_{S2}$. Experiments were conducted twice for each experimental condition (Run 1 and Run 2). Error bars indicate standard deviations.

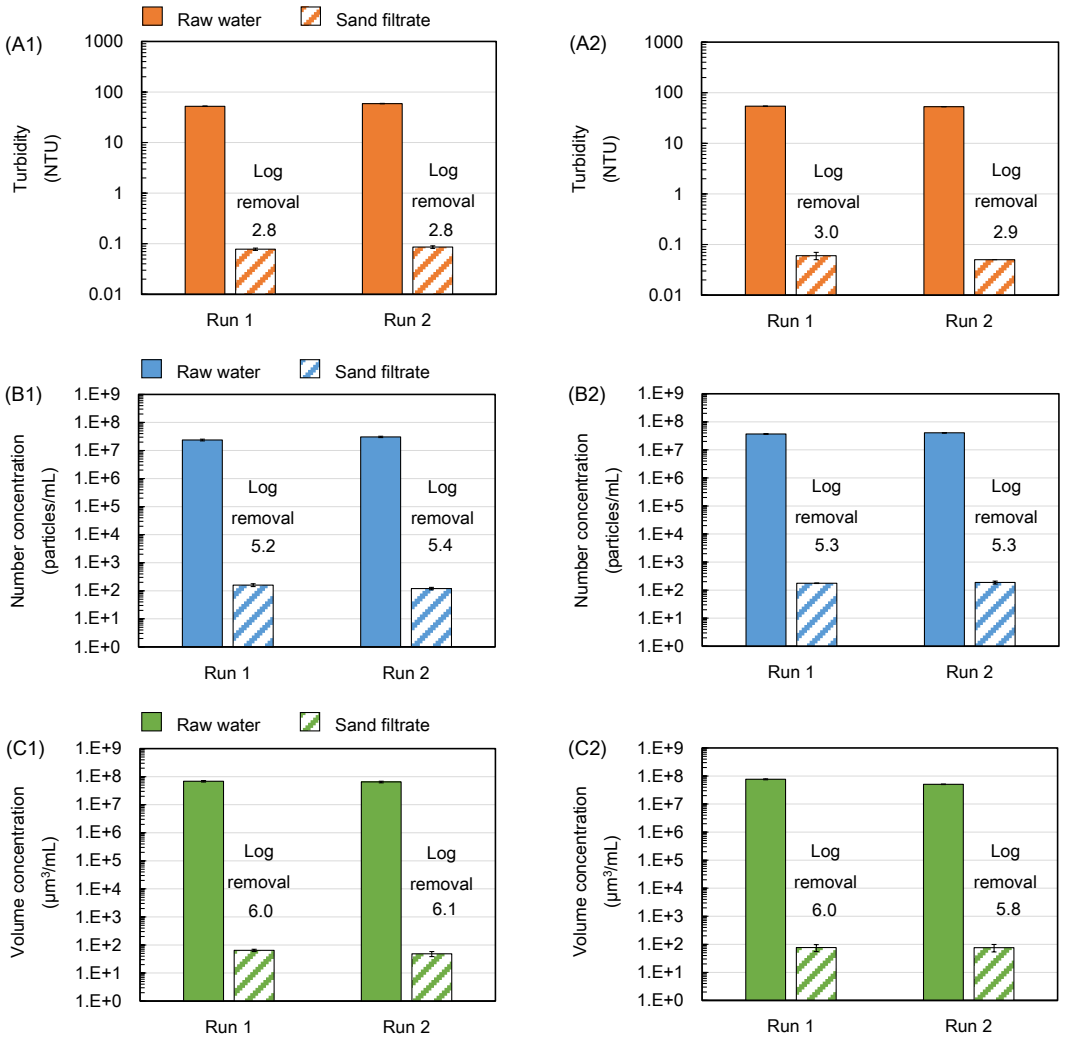

Figure 14S. Reduction of carbon particles by the CSF treatment. Panels A1–C1, river water (turbidity 5.7 NTU and DOC 0.9 mg/L) supplemented with $SPAC_{S2}$ at 7.5 mg/L; panels A2–C2, filtered tap water (turbidity < 0.07 NTU and DOC 0.5 mg/L) supplemented with $SPAC_{S2}$ at 7.5 mg/L. Experiments were conducted twice for each experimental condition (Run 1 and Run 2). Error bars indicate standard deviations of measurement for each experiment.

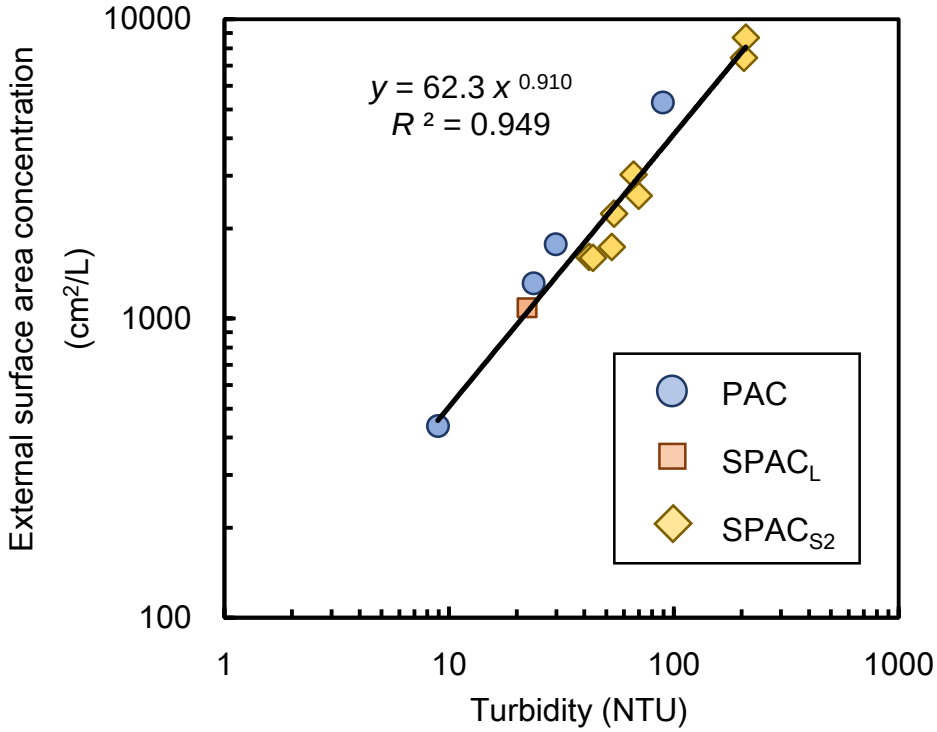

Figure 15S. External surface area concentration, as obtained by membrane-filtration and microscopic image analysis, versus turbidity. Standard suspensions of PAC (10, 30, and 80 mg/L), $SPAC_L$ (10 mg/L), and $SPAC_{S2}$ (6.0, 7.5, 10, and 30 mg/L).